LBL-35576
UC-410

Lawrence Berkeley Laboratory
UNIVERSITY OF CALIFORNIA

Accelerator & Fusion Research Division

Presented at the SRI '94 Conference, Upton, NY, July 18–22, 1994, and to be published in the Proceedings

Performance of a High Resolution, High Flux Density SGM Undulator Beamline at the ALS

T. Warwick, P. Heimann, D. Mossessian, W. McKinney, and H. Padmore

July 1994

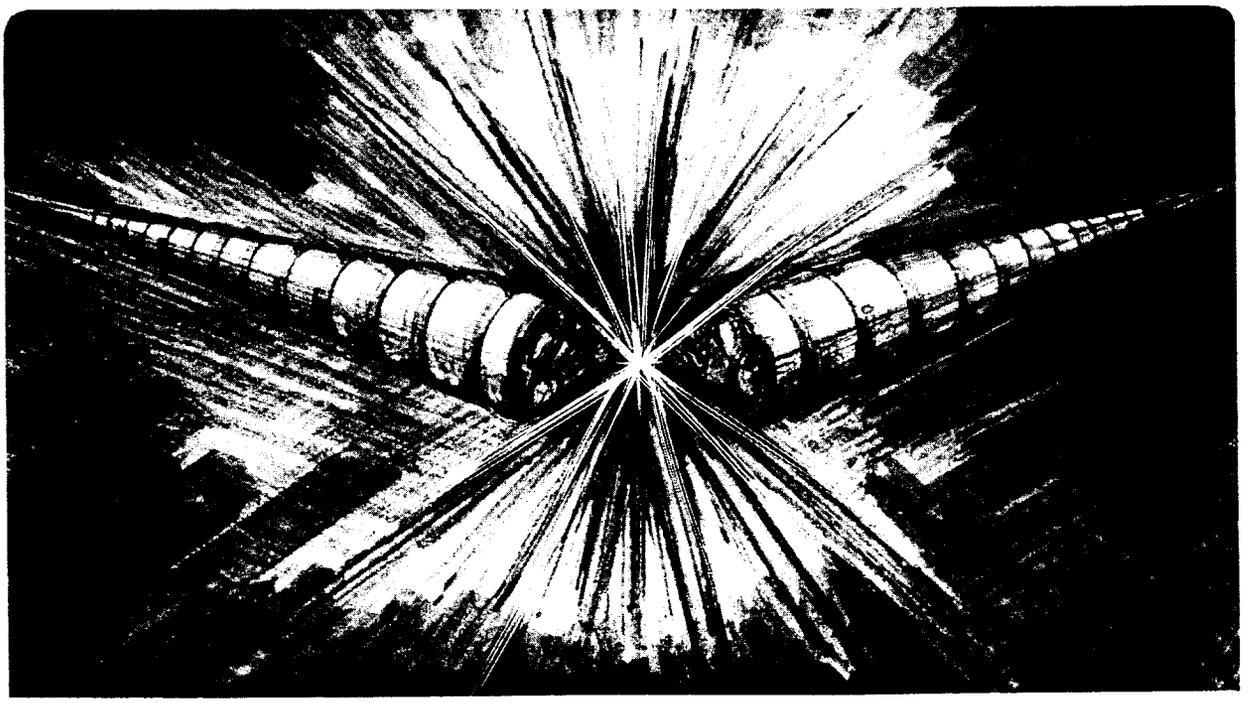

Prepared for the U.S. Department of Energy under Contract Number DE-AC03-76SF00098

LBL-35576
UC-410

PERFORMANCE OF A HIGH RESOLUTION, HIGH FLUX DENSITY SGM UNDULATOR BEAMLINE AT THE ALS

Tony Warwick, Phil Heimann, Dmitri Mossessian,
Wayne McKinney and Howard Padmore

Advanced Light Source
Accelerator and Fusion Research Division
Lawrence Berkeley Laboratory
University of California
Berkeley,CA 94720

July 15, 1994

***This work was supported by the Director, Office of Energy Research, Office of Basic Energy Sciences, Materials Sciences Division of the U.S. Department of Energy, under Contract no. DE-AC03-76SF00098**

Performance of a High Resolution, High Flux Density SGM Undulator Beamline at the ALS

Tony Warwick, Phil Heimann, Dmitri Mossessian,
Wayne McKinney and Howard Padmore.
Lawrence Berkeley Laboratory, Berkeley, CA 94720, USA

The performance of ALS beamline 7.0 is described. This is an integrated system for delivering radiation from a 5cm period undulator to spectroscopy and microscopy experiments across the range of photon energies from 60eV to 1200eV. The beamline is engineered to deliver the highest possible flux, with negligible deformation of the optic surfaces due to heating. Two experiment stations are served with rapid interchangeability. We report on the measured operational parameters, the resolution and flux delivered, and the refocus of the light into a small spot at the experiment.

1. INTRODUCTION

ALS beamline 7.0 (originally called ALS U5 beamline[1]) uses a state-of-the-art undulator source[2] with 89 magnetic periods of 5cm length. The beamline has operated in accordance with the design goals, with the undulator gap closing to 23mm, giving an operational range of deflection parameter values from K=0.5 to K=2.2. The beamline employs a spherical grating monochromator[3,4,5] with fixed entrance slit and sliding exit slit. Due to the single optical element between the slits and the simple single axis rotation, the SGM design is well suited to carry water cooled diffraction gratings. Apertures upstream reduce unnecessary heating of the optics so that water cooling within the substrates can eliminate the optical effects of heating. A bendable mirror images the exit slit to the experiment, giving a small spot across the operational range. The undulator gap can be changed as the grating rotates so that the beamline performs at the peaks of the undulator spectrum.

The commissioning was accomplished in three months during the spring of 1994. At present two of the three diffraction gratings are installed, and the scientific program is underway. Fluorescence and photo-electron spectroscopy experiments have been carried out, in which all of the resolved flux has been delivered to the sample within the field of view of the spectrometers, giving count rates higher than previously available. Photo-electron emission microscopy experiments have begun, with the illumination field matched to the microscope's acceptance. Scanning zone-plate microscopes are being developed.

The layout of optical components is shown in figure 1.

2. HORIZONTAL APERTURE, FIRST MIRROR AND ENTRANCE SLIT

Upstream of the first optic, an adjustable water cooled horizontal aperture removes up to 90% of the power at unwanted wavelengths in the sides of the beam. This aperture is precisely adjustable to pass the central cone and the resulting maximum transmitted power load (150 Watts) is the basis for the cooling design of the optical elements. The aperture can be placed off-axis horizontally, providing a broader spectral peak from the undulator, with lower peak flux, useful for near-edge photo-absorption spectroscopy.

The first undulator beamlines at the ALS include monochromators with entrance slits. There are two reasons. The first is to insure against possible source motion. The second is to further reduce the heat on the diffraction grating by absorbing high undulator harmonics in the first mirror and by absorbing light vertically off-axis on the slit.

The first mirror is carefully cooled by water flowing in internal channels[6,7] 3mm below the optical surface. Design calculations show that the mirror will suffer no appreciable thermal deformation. The required polishing tolerances have been met with measured r.m.s. slope errors less than 1μrad and r.m.s. surface roughness better than 6Å.

The radiation characteristics of the undulator have been comprehensively measured[8] and the device performs as expected. The beamline must always operate at the peaks of the undulator spectrum to produce the highest flux, it then operates with the radiation of the central cone on axis. This central cone has a maximum r.m.s. divergence of 75μrad, for the undulator fundamental at $K_{max}=4$.

A design goal for the beamline was to maximize the transmitted flux at the highest resolution of the monochromator. To optimize the transmission through the correspondingly narrow entrance slit, the first condensing mirror was designed with high demagnification (15:1), at the limit where increasing aberrations would reduce the flux transmitted through a 10μm slit. The divergence is increased by the same factor of 15 but the initial value is small enough that there is still no significant contribution to the resolution from the third order aberration at the grating, see below. (Actually, the only significant optical aberration in the entire beamline is this third order aberration, called coma or spherical aberration, which deflects the rays as the square of the aperture).

Figure 2. shows the vertical profile of the image made by the condensing mirror at the entrance slit. This measurement is obtained by pitching the mirror slightly and measuring, as a function of the mirror angle, the flux transmitted through the slit, set to 2μm wide. Two metal photo-diodes were used, one immediately behind the slit to measure the profile without wavelength selection, another beyond the exit slit of the monochromator, for measurements at selected wavelengths. One can see the aberrated image tail in the 'white' light, which fills the mirror. The tail is reduced when the wavelength of the central cone is selected, because the divergence is small and only the center of the mirror is illuminated. The tail

returns if the monochromator is tuned to select wavelengths off-axis. All the radiation in the central cone can be transmitted through a 30μm slit and with a 10μm slit the transmission is between 50% and 70%, depending on the K value and the corresponding undulator divergence. The entrance slit is engineered[9] to deform by less than 2μm under the full heat load (9.5W per horizontal mm, 330 W mm^{-2} peak)

3. DIFFRACTION GRATINGS

The diffraction gratings are the result of a collaboration between ALS, APS, Photon Sciences, Rocketdyne and Hughes Corporation.[10] The grating substrates are brazed 'glidcop' assemblies with internal water channels and a polished coating of electroless nickel. They were coated with photo-resist, exposed holographically, etched and the grooves were ion milled into the nickel. The final result was square wave profile grooves in the nickel. This profile was chosen as the best compromise between ease of fabrication, higher order cancellation and broad band efficiency. Groove depths were chosen by calculation with exact electromagnetic theory[11].

Figure 3. shows a long trace profiler[12] (LTP) trace of one of the grating blanks. Residual slope variation is plotted after subtraction of the best fit circle. These data were taken in 1992. Even including the wide low frequency excursions and the higher frequency ringing which were later shown to be due to systematic errors in the LTP, the r.m.s. deviation from spherical is only 1.1 μrad. The efficiency of the gratings were measured with the laser plasma source, monochromator and reflectometer in the Center for X-Ray Optics at LBL. Excellent stray light and efficiency uniformity were obtained[13].

4. SPECTRAL RESOLUTION

This design has the entrance slit held fixed in the fixed illumination from the condensing mirror so that the SGM is no longer a Rowland circle instrument. The third order geometric aberration from the grating is then not zero, except at the one wavelength where the monochromator motion crosses the Rowland circle. Still, the aberration contributes no more to degrading the resolution than do the polisher's slope errors on the grating surface. Figure 4. shows the computed contributions of these slope errors (assuming 0.5 μrad r.m.s.), and of the grating third order aberration, for the ray at the half maximum of the illumination pattern. We expect a resolving power of at least 8,000 at all wavelengths.

Figure 5. shows a verification of the resolving power. This nitrogen $1s-\pi^*$ photo-absorption spectrum has become the benchmark for high resolution soft x-ray beamlines. The data are fit with a natural linewidth[14] of 128meV and show and show a resolving power in excess of 8,000. This was achieved without any re-alignment after installation of the diffraction

gratings and slits. Careful fiducialization and survey and a well thought out grating installation scheme[15], in which the grooves are set parallel to the rotation axis (which is precisely horizontal) by checking diffracted orders from a HeNe laser, gave excellent alignment. The nitrogen spectrum was measured by recording the ion current from a gas cell 20cm long at a pressure of 10mTorr, with the photon beam entering through an aluminum window 100nm thick.

5. RESOLVED FLUX AND SPOT SIZE

The resolved flux is measured after the last optical element by recording the photo-current from a freshly evaporated gold grid. The quantum efficiency of gold at the appropriate wavelength is taken from the literature[16]. Figure 6. shows the expected values from a computation which includes the effects of reflectivity and diffraction efficiency of the optics and the geometric transmission factors, including aberrations. Data points measured at the peaks of the undulator spectra are superimposed.

The computations shown in figure 6. include neither the effects of undulator field errors nor of the energy spread of the electron beam.

The undulator field errors are not significant for the first grating using the 1st undulator harmonic. For the third grating using the undulator fifth harmonic they should reduce the flux below the computed values by about 25%[17].

The natural energy spread of the electron beam has been extracted from the measured spectral widths of the undulator harmonics at low current (0.6mA). A value is obtained for the FWHM:

$$\delta\gamma/\gamma \approx 2 \times 10^{-3}$$

This is in agreement with accelerator design calculations. It should broaden the spectrum and reduce the flux at the peak of the 5th harmonic of the undulator spectrum by a factor of about 2. The FWHM spectral width is given by:

$$(\delta\omega/\omega)^2 \approx (1/nN)^2 + (2\,\delta\gamma/\gamma)^2$$

where N is the number of periods in the undulator (N=89) and n is the harmonic number (n=5).

The discrepancies between the computations and the flux measurements using the third and fifth harmonics are partly due to these two effects. They are also due to the additional large time-average energy spread presently observed as a result of undamped coupled bunch oscillations at high current in the storage ring. A longitudinal damping system designed to reduce the energy spread at high current to the values measured at low current has been tested[18] and will become active in August 1994.

A focused spot at the experiment is produced by refocus mirrors which image the exit slit with approximately unity magnification in the vertical direction and produce a 14:1 demagnified image of the electron beam in the horizontal direction. The vertical refocus mirror has a variable focal length, so that the exit slit can always be re-focused as it moves longitudinally to stay at the focus of the grating[19]. Figure 7. shows the spot size measured by scanned photo-emissive knife edges with the exit slit 30μm wide. This spot is typical of the bandwidth and illumination delivered to an emission spectroscopy or emission microscopy experiment. All of the resolved flux is delivered into this spot across the full range of beamline operation.

7. FUTURE DIRECTIONS FOR BEAMLINES AT THE ALS

Beamline 7.0 has been a great success, the simple SGM design has lent itself well to the complex task of engineering the cooled optics and the commissioning has been accomplished quickly. For the future, this SGM design has two disadvantages, moving exit slits and the need for several gratings. We are considering other designs for future beamlines which span the required range of wavelength with fewer gratings and have stationary slits

The excellent stability of the electron beam in the ALS storage ring will allow us to build entrance slit-less monochromators in the future, with the advantage of simplicity and increased overall efficiency. The main challenge for these soft x-ray undulator lines will be to maintain the high resolution with increased heat load on the diffraction grating.

ACKNOWLEDGMENTS

This paper represents the excellent work of many people at the ALS over a period of several years, particularly the members of the beamline engineering group under Dick DiGennaro.

This work was supported by the Director, Office of Energy Research, Office of Basic Energy Sciences, Materials Sciences Division of the U.S.Department of Energy, under Contract No. DE-AC03-76SF00098

REFERENCES

1. T. Warwick and P. Heimann, Nucl. Instr. Meth. Phys. Res. A319 (1992) 77

2. E. Hoyer, J. Akre, J. Chin, W. Gath, W. V. Hassenzahl, D. Humphries, B. Kincaid, S. Marks, P.Pipersky, D. Plate, G. Portmann, R. Schlueter, these proceedings.

3. C. T. Chen and F. Sette, Rev. Sci. Instr. 60 (1989) 1616

4. H. Hogrefe, M. R. Howells and E. Hoyer, SPIE 733 (1987) 274

5. K. J. Randall, W. Eberhardt, J. Feldhaus, W. Erlebach, A. M. Bradshaw, Z. Xu, P. D. Johnson and Y. Ma, Nucl. Instr. Meth. Phys. Res. A319 (1992) 101

6. R. Digennaro and T. Swain, Nucl. Instr. Meth. Phys. Res. A291 (1990) 305

7. R. Digennaro and T. Swain, Nucl. Instr. Meth. Phys. Res. A291 (1990) 313

8. P. Heimann, D. Mossessian, T. Warwick, E. Gullikson, C. Wang, S. Marks, H. Padmore, these proceedings.

9. N. C. Andresen, private communication

10. W. R. McKinney, C. L. Shannon and E. Shults, Nucl. Instr. Meth. Phys. Res. A347 (1993) 220

11. S. V. Valdes, W. R. McKinney and C. Palmer, Nucl. Instr. Meth. Phys. Res. A347 (1993) 216

12. S. C. Irick, SPIE, 1720 (1992) 162

13. W. McKinney, D. Mossessian, E. Gullikson and P. Heimann, these proceedings.

14. G. C. King, F. H. Read and M. Tronc, Chem. Phys. Lett., 15 (1977) 50.

15. W. R. McKinney, M. R. Howells, T. Lauritzen, J. Chin, R. DiGennaro, E. Fong, W. Gath, J. Guigli. H. Hogrefe, J. Meneghetti, D. Plate, P. A. Heimann, L. Terminello, Z. Ji, D. A. Shirley and F. Senf, Nucl. Instr. Meth. Phys. Res. A291 (1990) 221

16. R. H. Day, P. Lee, E. B. Saloman and D. J. Nagel, J. Appl. Phys., 52 (1981) 6968.

17. S. Marks, D. Humphries, B. Kincaid, R. Schlueter and C. Wang, SPIE, 2013 (1993) 171.

18. J. Corlett, private communication

19. T. Warwick, M. Howells and M. Shlezinger, these proceedings.

FIGURE CAPTIONS

Figure 1. Layout of the optical components for ALS beamline 7.0, showing mirror lengths and radii and distances from the source in meters. All optics are spherical or cylindrical.

Figure 2. The vertical image of the undulator source at the entrance slit. The upper part of the figure is measured using the 'white' light. The lower part is measured through the monochromator at photon energies a) in the central cone so that the third order mirror aberration is less and b) off-axis, so that the ends of the mirror are used and the aberration is worse.

Figure 3. Slope errors measured on one of the diffraction gratings using the LBL long trace profiler.

Figure 4. The computed contributions to the resolution from a) the third-order aberration at the grating and b) the grating slope error, assuming an r.m.s. value of 0.5μrad.

Figure 5. Nitrogen 1s-π^* photo-absorption spectrum showing vibrationally resolved states. The monochromator resolving power is in excess of 8,000.

Figure 6. Computed and measured values of the resolved flux. These computations are with the monochromator slits set for a nominal resolving power of 10,000. The three gratings are used with the first, third and fifth harmonics from the undulator, respectively. Measured values are superimposed, corrected for the slit widths (≈10μm) and the electron current (400mA) used in the calculations. The computations include neither the effects of undulator field errors nor the effects of the energy spread of the electron beam.

Figure 7. Measured spot size at the experiment after refocus. The measurements were made by vertical and horizontal scanning knife-edges before the installation of the experiment chambers.

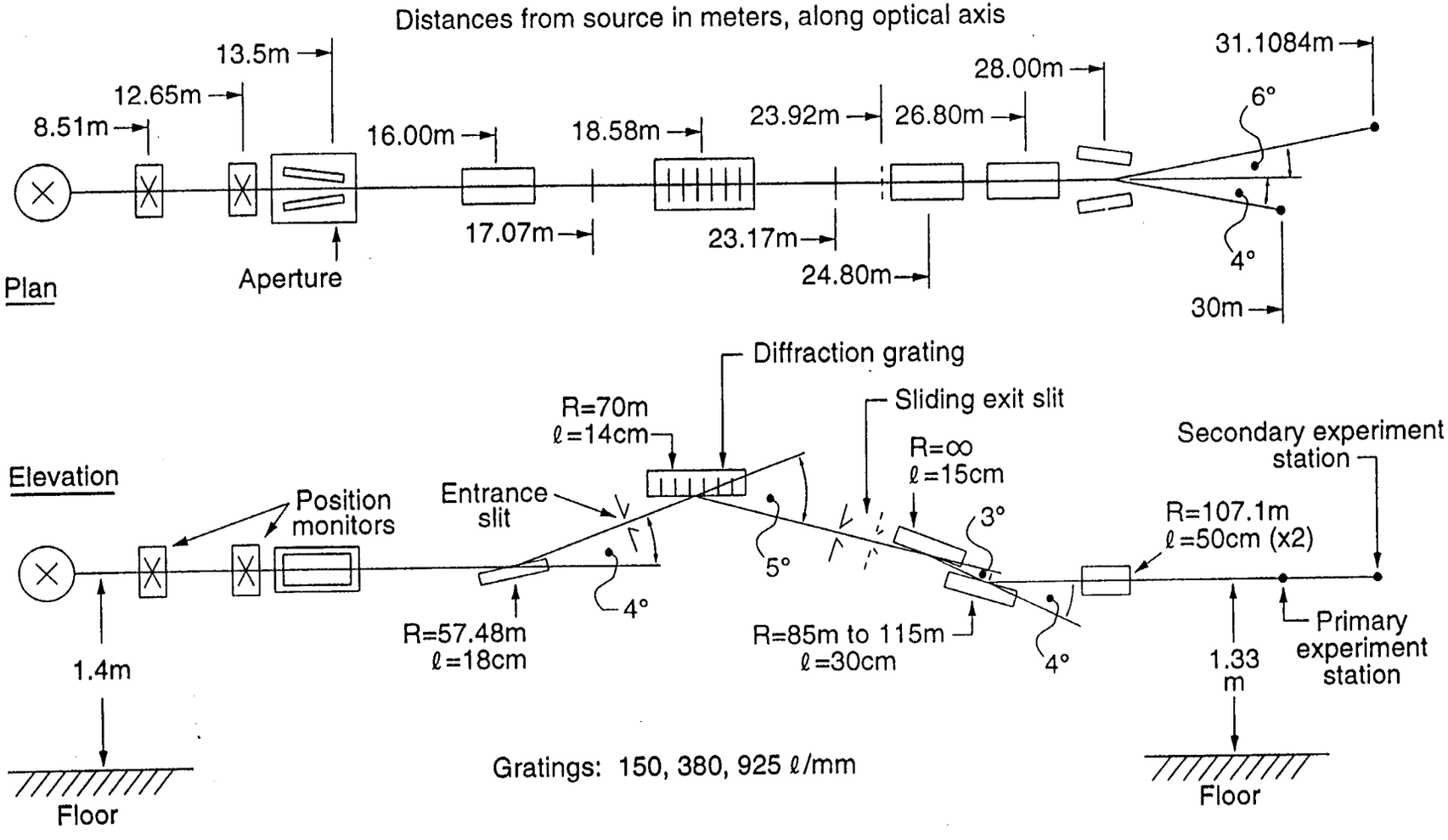
Distances from source in meters, along optical axis
8.51m
12.65m
13.5m
16.00m
17.07m
18.58m
23.17m
23.92m
24.80m
26.80m
28.00m
31.1084m
30m
6°
4°
Plan
Aperture
Elevation
Position monitors
Entrance slit
R=70m
ℓ=14cm
Diffraction grating
Sliding exit slit
R=∞
ℓ=15cm
Secondary experiment station
R=107.1m
ℓ=50cm (x2)
3°
5°
4°
4°
R=57.48m
ℓ=18cm
R=85m to 115m
ℓ=30cm
1.4m
1.33 m
Primary experiment station
Floor
Floor
Gratings: 150, 380, 925 ℓ/mm

XBL 947-4507

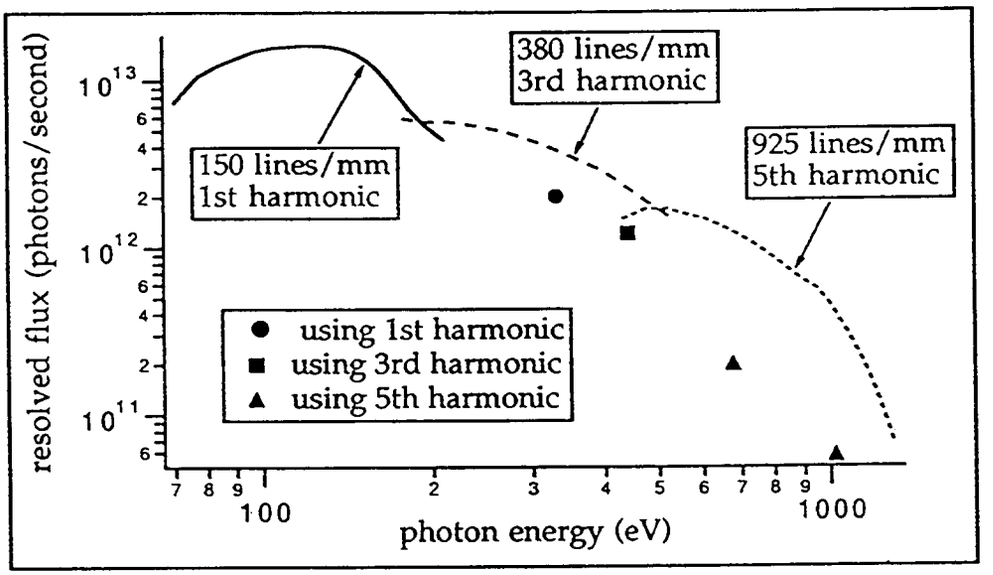
resolved flux (photons/second)
10^{13}
10^{12}
10^{11}
6
4
2
380 lines/mm
3rd harmonic
925 lines/mm
5th harmonic
150 lines/mm
1st harmonic
using 1st harmonic
using 3rd harmonic
using 5th harmonic
7 8 9
100
2 3 4 5 6 7 8 9
1000
photon energy (eV)

XBL 947-491

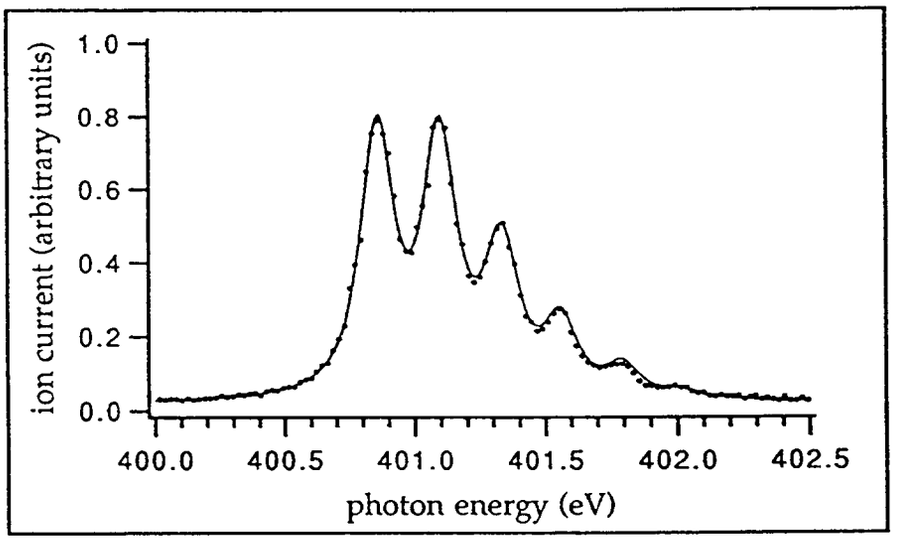
ion current (arbitrary units)
1.0
0.8
0.6
0.4
0.2
0.0
400.0
400.5
401.0
401.5
402.0
402.5
photon energy (eV)

XBL 947-490

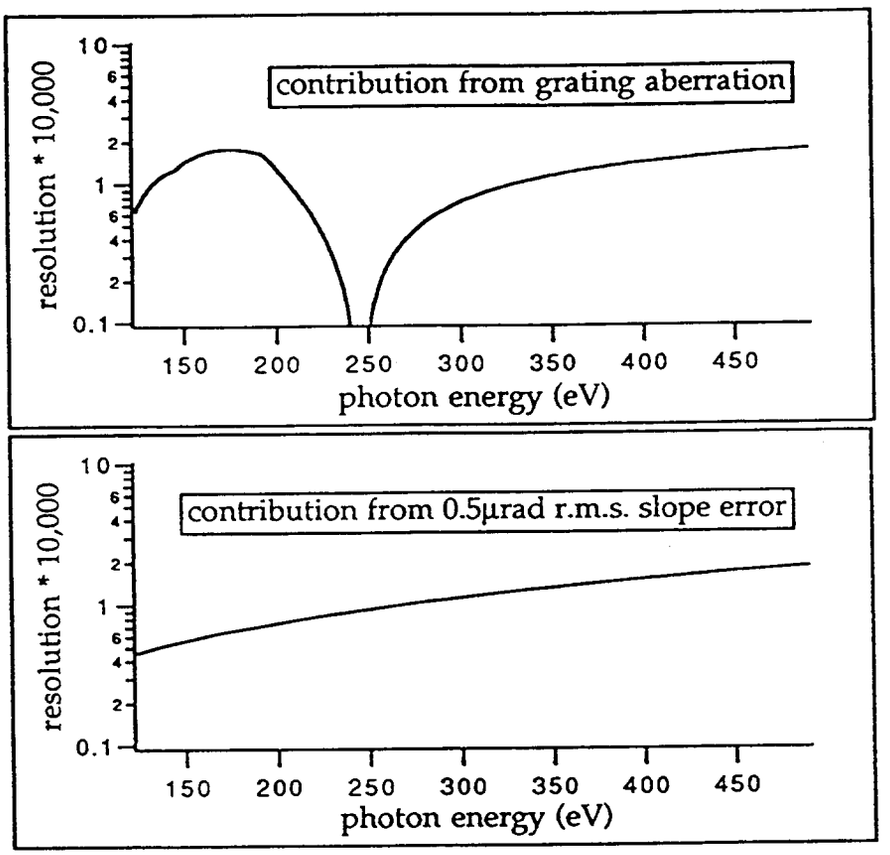
contribution from grating aberration
resolution * 10,000
10
6
4
2
1
6
4
2
0.1
150
200
250
300
350
400
450
photon energy (eV)
contribution from 0.5μrad r.m.s. slope error
resolution * 10,000
10
6
4
2
1
6
4
2
0.1
150
200
250
300
350
400
450
photon energy (eV)

XBL 947-487

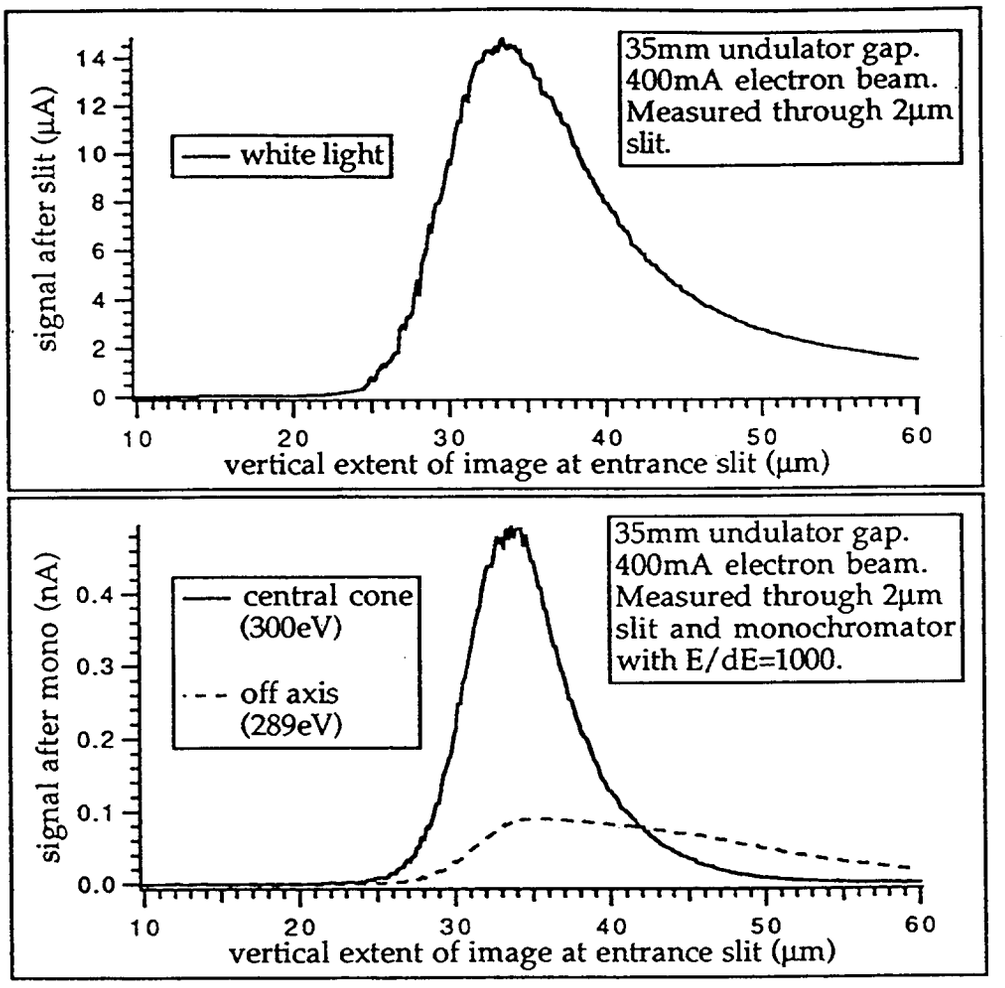
35mm undulator gap.
400mA electron beam.
Measured through 2μm slit.
white light
signal after slit (μA)
vertical extent of image at entrance slit (μm)
35mm undulator gap.
400mA electron beam.
Measured through 2μm slit and monochromator with E/dE=1000.
central cone (300eV)
off axis (289eV)
signal after mono (nA)
vertical extent of image at entrance slit (μm)

XBL 947-488

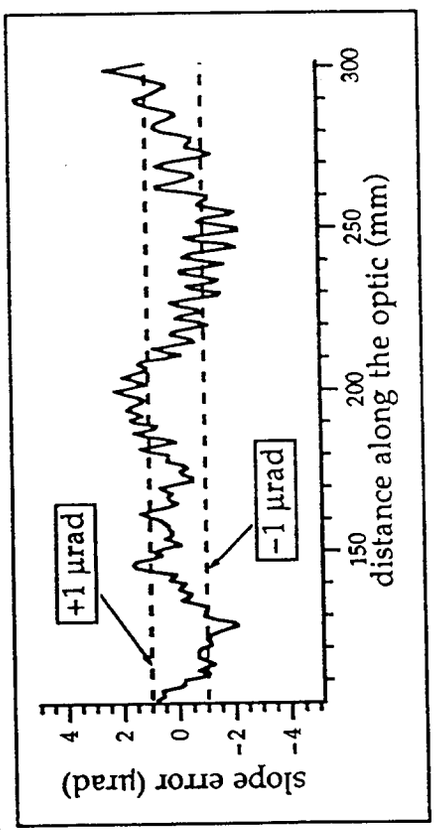
slope error (μrad)
4
2
0
-2
-4
+1 μrad
-1 μrad
150
200
250
300
distance along the optic (mm)

XBL 947-489